Atmospheric Environment 136 (2016) 43–53

Contents lists available at ScienceDirect

Atmospheric Environment

journal homepage: www.elsevier.com/locate/atmosenv

Benefits of China's efforts in gaseous pollutant control indicated by the bottom-up emissions and satellite observations 2000–2014

Yinmin Xia [a], Yu Zhao [a, b, *], Chris P. Nielsen [c]

[a] State Key Laboratory of Pollution Control & Resource Reuse and School of the Environment, Nanjing University, 163 Xianlin Ave., Nanjing, Jiangsu 210023, China
[b] Jiangsu Collaborative Innovation Center of Atmospheric Environment and Equipment Technology (CICAEET), Nanjing University of Information Science & Technology, Jiangsu 210044, China
[c] Harvard China Project, School of Engineering and Applied Sciences, Harvard University, 29 Oxford St, Cambridge, MA 02138, USA

HIGHLIGHTS

- The trends in emissions and VCDs match well in China except for SO_2.
- The recent controls prove more effective than those in earlier years except for CO.
- Coal consumption dominated the growth of NO_X emissions and NO_2 VCDs till 2012.
- The effects of air pollution controls differed by region and species in the country.
- Varied emissions from specific sources are evaluated through satellite observation.

ARTICLE INFO

Article history:
Received 10 December 2015
Received in revised form
7 April 2016
Accepted 11 April 2016
Available online 12 April 2016

Keywords:
Emission control
Inter-annual trends
Vertical column density
China

ABSTRACT

To evaluate the effectiveness of national air pollution control policies, the emissions of SO_2, NO_X, CO and CO_2 in China are estimated using bottom-up methods for the most recent 15-year period (2000–2014). Vertical column densities (VCDs) from satellite observations are used to test the temporal and spatial patterns of emissions and to explore the ambient levels of gaseous pollutants across the country. The inter-annual trends in emissions and VCDs match well except for SO_2. Such comparison is improved with an optimistic assumption in emission estimation that the emission standards for given industrial sources issued after 2010 have been fully enforced. Underestimation of emission abatement and enhanced atmospheric oxidization likely contribute to the discrepancy between SO_2 emissions and VCDs. As suggested by VCDs and emissions estimated under the assumption of full implementation of emission standards, the control of SO_2 in the 12th Five-Year Plan period (12th FYP, 2011–2015) is estimated to be more effective than that in the 11th FYP period (2006–2010), attributed to improved use of flue gas desulfurization in the power sector and implementation of new emission standards in key industrial sources. The opposite was true for CO, as energy efficiency improved more significantly from 2005 to 2010 due to closures of small industrial plants. Iron & steel production is estimated to have had particularly strong influence on temporal and spatial patterns of CO. In contrast to fast growth before 2011 driven by increased coal consumption and limited controls, NO_X emissions decreased from 2011 to 2014 due to the penetration of selective catalytic/non-catalytic reduction systems in the power sector. This led to reduced NO_2 VCDs, particularly in relatively highly polluted areas such as the eastern China and Pearl River Delta regions. In developed areas, transportation is playing an increasingly important role in air pollution, as suggested by the increased ratio of NO_2 to SO_2 VCDs. For air quality in mega cities, the inter-annual trends in emissions and VCDs indicate that surrounding areas are more influential in NO_2 level for Beijing than those for Shanghai.

1. Introduction

Due to tremendous growth of the economy and fossil fuel

* Corresponding author. State Key Laboratory of Pollution Control & Resource Reuse and School of the Environment, Nanjing University, 163 Xianlin Ave., Nanjing, Jiangsu 210023, China.
E-mail address: yuzhao@nju.edu.cn (Y. Zhao).

http://dx.doi.org/10.1016/j.atmosenv.2016.04.013
1352-2310/

consumption, China has been suffering from severe air pollution for decades (Zhang et al., 2012). Based on satellite observations and chemical transport simulations, the highest of tropospheric NO_2 in the world have been indicated in eastern China, the region with the largest densities of population and economic activity in the country (Richter et al., 2005). Existing emission inventories indicate that China is the dominant source of gaseous pollutants including SO_2, NO_X and CO in Asia (Streets et al., 2003; Zhang et al., 2009; Cofala et al., 2007; Kurokawa et al., 2013).

Facing the big challenge of improving air quality, China undertook a series of measures to improve energy efficiency and to reduce emissions during the 11th Five-Year Plan (11th FYP) period (2006–2010). Small industrial boilers and kilns with low energy efficiency were gradually shut down or replaced with larger ones featuring advanced dust collectors. Installation of flue gas desulfurization (FGD) systems has been required for all new thermal power units since 2005. At the same time, the fraction of washed coal has increased from 33% in 2005 to 51% in 2010 (Wang and Hao, 2012). These measures are thought to have been effective: national emissions of SO_2 and particulate matter (PM) were officially reported to decline by 14% and 30% from 2005 to 2010, respectively (MEP, 2011). Other studies with more conservative assumptions have likewise suggested substantial benefits of emission controls, particularly for SO_2 and CO (Lu et al., 2011; Zhao et al., 2012a, 2013).

The measures in 11th FYP, however, failed to restrain the growth of NO_X emissions that are critical to formation of $PM_{2.5}$ and O_3 in the atmosphere (Zhao et al., 2013). Big challenges on air quality improvement still existed over the country (Wang and Hao, 2012). During the 12th FYP period (2011–2015), China aimed to reduce the annual emissions of SO_2 and NO_X by 8% and 10% compared to 2010, respectively. More stringent measures were taken to control NO_X emissions, including the use of selective catalytic/non-catalytic reduction (SCR/SNCR) systems in the power sector and staged implementation of tighter emission standards on vehicles. Moreover, a series of new standards with aggressive emission limits for power, cement, and the iron & steel industries have been issued successfully since 2011. Those measures are believed to have helped achieve national targets of emission abatement, but their impacts on emissions and air quality have been seldom quantified.

In this study, the emissions of gaseous pollutants in China are estimated using bottom-up methods for the most recent 15 years (2000–2014), in order to examine the effectiveness of national air pollution control policies, particularly for the years after 2010. Vertical column densities (VCDs) from satellite observation are used to evaluate inter-annual trends and the spatial distribution of emissions, and temporal and spatial patterns of ambient levels of gaseous pollutants across the country. By combining the information of emissions and satellite observations, the impacts of controls on given source types are analyzed, and the source contributions to air quality for two developed mega cities and their surrounding regions are further identified.

2. Data and methods

2.1. Emission inventory

China's annual emissions of SO_2, NO_X, CO and CO_2 are estimated from 2000 to 2014 using bottom-up methods described in previous studies (Zhao et al., 2011, 2012a, 2012b, 2013). Anthropogenic emission sources include four main categories: thermal power plants (TPP, including both electricity generation and heat production), all other industry (IND), transportation (TRA, including on-road and non-road subcategories), and the residential & commercial sector (RES, including fossil fuel and biomass combustion subcategories). IND is further divided into cement production (CEM), iron & steel plants (ISP), other industrial boilers (OIB), and other non-combustion processes (PRO), reflecting the structure of available data. In general, the annual emissions of each species are calculated by province using Eq. (1) and are then aggregated to national level:

$$E_{i,j,t} = \sum_k \sum_m \sum_n AL_{j,k,m,n,t} \times EF_{i,j,k,m,t} \times R_{i,j,k,m,t} \times \left(1 - \eta_{i,n,t}\right) \tag{1}$$

where i, j, k, m, n and t stand for species, province, sector, fuel type, emission control technology, and year, respectively; AL is the activity level, either energy consumption or industrial/agricultural production; EF is the unabated emission factor; R is the penetration rate of the relevant emission control technology; and η is the removal efficiency of that technology.

The activity levels are compiled mainly from Chinese official energy (NBS, 2013a, 2014) and industrial economic statistics (NBS, 2013b, 2014), as discussed in our previous work (Zhao et al., 2013). Detailed data on energy budgets by province for 2013 and 2014 were unavailable at the time of writing and thus the national fast-track statistics for these two years had to be used to extrapolate provincial activity levels by applying consistent provincial shares with 2012.

Emission factors, expressed as the pollutant emissions per unit of activity, have changed significantly during the study period, particularly for power, transportation, and certain industrial sectors including cement and iron & steel production, as a series of successive air pollution control measures have been implemented. In this work, two cases, "primary" (PRI) and "standard" (STD), are developed to represent the inter-annual trends in emission factors and thereby emissions. Following the method in our previous work (Zhao et al., 2013), PRI case analyzes the penetrations of advanced combustors with improved energy efficiency and air pollutant control devices (APCDs) with improved pollutant removal efficiency. As shown in Fig. S1 in the supplement, the increased use of advanced combustors and APCDs is assumed to have led to continuously reduced emission factors for most emission sources and pollutant species, with a few exceptions such as NO_X from cement kilns (Lei et al., 2011) and from heavy-duty vehicles (Yao et al., 2011; Wu et al., 2012). In addition to PRI case, STD case is developed to re-estimate the SO_2 and NO_X emissions for 2011–2014 (i.e., there is no difference between the two cases for SO_2 and NO_X emissions for 2000–2010 and for other species for 2000–2014). This case optimistically assumes that the series of emission standards for power and industrial sectors issued or updated since 2011 (listed in Table S1 in the supplement) have been strictly enforced. All of the tightened emission limits and schedules of implementation are assumed to be met, for both existing and new emission sources (Zhao et al., 2014). Based on the emission limits from the standards, emission factors from the power, cement, iron & steel and non ferrous metal smelting industries are estimated to have declined further in STD compared to those in the PRI case, as summarized in Table S2 in the supplement.

2.2. Satellite data

Satellite observations can provide information on temporal trends and spatial patterns of atmospheric chemistry composition and concentrations of pollutants of concern. In this work, the VCDs of NO_2, SO_2, and CO from various satellite retrieval products are used to evaluate the anthropogenic emissions and the effects of pollution control policies.

The Ozone Monitoring Instrument (OMI) aboard the EOS Aura satellite is an ultraviolet/visible nadir solar backscatter spectrometer which was set in a sun-synchronous polar orbit at an altitude of 705 km with a local equator crossing time of 13:45 on the ascending node. OMI provides data for key air quality components including NO_2, SO_2, BrO, HCHO, and aerosol, which are observed based on the Differential Optical Absorption Spectroscopic (DOAS) technique. In this work, the VCDs of tropospheric NO_2 are taken from OMI, retrieved by the Royal Netherlands Meteorological Institute (KNMI), and the monthly data with spatial resolution of $0.125^\circ \times 0.125^\circ$ are used (data source: http://www.temis.nl/airpollution/no2col/no2regioomimonth_v2.php). Tropospheric NO_2 over China in this product is consistent with NO_2 data from ground-based measurements with multi-axis DOAS ($R^2 = 0.96$; Lin et al., 2014). For SO_2, OMI data of daily planetary boundary layer (PBL) VCDs in the OMSO2 Level-3 products are acquired from NASA's Goddard Earth Sciences Data and Information Services Center (GES-DISC) at http://disc.sci.gsfc.nasa.gov/Aura/data-holdings/OMI/omso2e_v003.shtml, with spatial resolution of $0.25^\circ \times 0.25^\circ$. Monthly average PBL VCDs are then calculated from the daily data product. Since clouds reduce the accuracy of satellite measurements, only pixels with radiative cloud fraction$\leq$0.2 have been analyzed in this study. Lee et al. (2009) compared SO_2 VCDs from OMI with those from a global atmospheric chemistry model (GEOS-Chem) (R = 0.81 in eastern China) and evaluated the total error at 44%–80% in China.

CO is measured by multiple space-based instruments including Measurement of Pollution in the Troposphere (MOPITT), Atmospheric Infra Red Sounder (AIRS), Scanning Imaging Absorption Spectrometer for Atmospheric CHartographY (SCIAMACHY), and the Infrared Atmospheric Sounding Interferometer (IASI). MOPITT product version 5 (Deeter et al., 2013; Worden et al., 2013) is used in this study. The monthly mean of CO total columns at spatial resolution of $1^\circ \times 1^\circ$ are obtained from the MOPITT multi-spectral retrievals combining thermal-infrared and near-infrared channels (http://reverb.echo.nasa.gov/reverb/datasets#utf8=%E2%9C%93&spatial_type=rectangle). Pixels with cloud fraction$\leq$0.05 are passed on to the retrieval algorithm by the V5 cloud detection algorithm. The bias drift in total column retrieval is about 0.08×10^{18} molecules/cm^2 (2–4%) (Deeter et al., 2013).

Due to the relatively large solar zenith angle and possible snow cover, large uncertainty may exist in satellite data for winter. Additionally, the long lifetime of SO_2 and NO_2 in winter makes the pollution plums transport long distance, leading to bias when the VCD data are used for indicating the primary emissions. Without using the data for the whole year, however, monthly or seasonal variations of VCDs that might result partly from anthropogenic activities (e.g., enhanced heating in winter, and limited industry and energy use attributed to Beijing Olympics, 2008 and the economic crisis afterwards) could not fully be captured. In this work, therefore, the 12-month moving averages are used for the inter-annual time series analysis (Section 3.2), and both the data for full year and those for May–September are used for the analysis of spatial variation over the country (Section 4.1 and 4.3).

3. Time-series analysis of national emission controls

3.1. Inter-annual trends in bottom-up emissions

Fig. 1 shows the national emissions of SO_2, NO_X, CO, and CO_2 from 2000 to 2014 (see Table S3 in the supplement for detailed numbers). With limited measures to reduce emission factors, the CO_2 emissions are estimated to have increased continuously and can indicate the growth of fossil fuel consumption. The share of total CO_2 emissions produced by coal-fired power plants has increased from 30% in 2000 to 36% in 2014, while that of the residential and commercial sector have decreased from 26% to 14%, indicating the fast increased electricity demand of the country and slower growth in household use of solid fuel (Fig. 1d). SO_2 emissions are estimated to have increased from 18.2 million metric tons (Mt) in 2000 to 30.0 Mt in 2006 and then to have decreased to 26.4 Mt in 2010. In the PRI case, very small inter-annual variability in SO_2 emissions were found after 2011 (Fig. 1a). As the largest SO_2 source, the thermal power share of total emissions decreased from 62.7% in 2005 to 38.4% in 2014 while its share of CO_2 emissions varied little, indicating key role of this sector in reducing SO_2 emissions since 2005 due to increased use of FGD. The emission trends of NO_X and CO_2 are similar before 2011, implying that NO_X emissions were dominated by energy growth and little change in emission factors during 2000–2010. NO_X emissions are estimated to have increased from 11.7 Mt in 2000 to 29.8 Mt in 2011, and then to have decreased to 27.7 Mt in 2014 (Fig. 1b). Reduction of NO_X emissions is generally attributed to controls at coal-fired power plants, due to increased and improved use of SCR/SNCR, while emissions from other sectors continued to increase. In 2010, TPP and IND are estimated to have contributed larger fractions of national SO_2 emissions (41% and 44%, respectively) than of NO_X (39% and 28%), while TRA contributed little to SO_2 emissions (1%) but considerably to NO_X (25%).

Fig. 1 also shows the estimated emissions of SO_2 and NO_X in the STD case since 2011 and 2012, respectively. Note the emission standards for non ferrous metal smelting since late 2010 have little impact on NO_X control, as shown in Table S1. The differences in annual emissions for the two cases (calculated as (PRI-STD)/PRI) range 7–16% for SO_2 and 4–8% for NO_X during 2012–2014. Emissions by sector and year for the two cases are summarized in Table 1. From 2011 to 2014, SO_2 emissions are calculated to have decreased 19% in the STD case but only 5% in the PRI one, implying considerable benefits of the emission standards if fully implemented (note the reduction rate from 2005 to 2010 is estimated at 9% in this work). Although penetration of FGD systems in TPP increased faster during 2005–2010 (Zhao et al., 2014), the larger abatement of SO_2 emissions found in the later years of the STD case would be attributed mainly to: 1) improved operation and removal efficiency of FGD in the power sector as required by the relevant emission standard (GB13223-2011), which was in question for the 11th FYP period (Xu, 2011; Zhao et al., 2013); and 2) effective controls in certain other industrial sources after 2010. As can be found in Table 1, the differences in emissions from TPP, ISP, and PRO (dominated by nonferrous metal smelting) between the two cases are 2596 kilo tons (kt, 26% relative to the PRI case), 558 kt (25%), and 831 kt (21%), respectively, in 2014. The NO_X emissions decrease 9% from 2010 to 2014 in the STD case, i.e., at a lesser rate than that of SO_2. TPP is the sector with the biggest NO_X emission difference between the two cases, at 2031 kt (27% relative to the PRI case) for 2014. The benefits of emission standards for CEM and ISP are less, attributed partly to later implementation of those standards.

Different from SO_2 and NO_X, CO released from TPP is limited, and RES and ISP play much more important roles in CO emissions (Fig. 1c). National emissions increased 38% from 127 Mt in 2000 to176 Mt in 2005, with the growth dominated by ISP, for which the emission share increased from 13% to 19%. The inter-annual variability in emissions from 2005 to 2014 was relatively small, with the peak in annual emissions estimated at 184 Mt in 2010. Meanwhile, the ratio of CO to CO_2 decreased 41%, implying significant improvement in combustion efficiency.

Besides this work, studies with multiple years of results are collected and compared to examine the inter-annual trends in China's national emissions, as shown in Fig. 1. For most cases, however, this comparison can only be conducted for years before 2010, as estimates after 2010 are unavailable for most studies

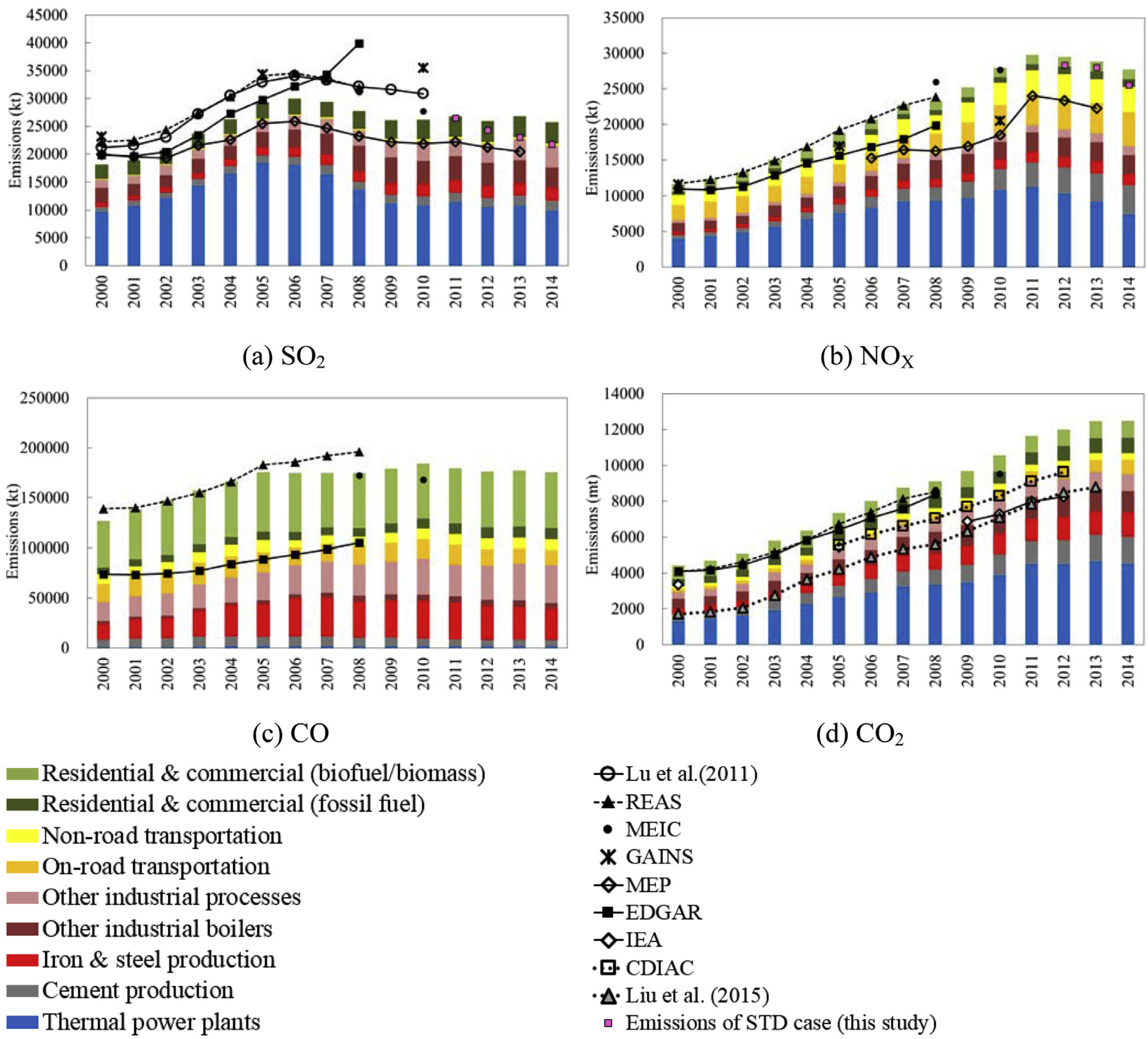

Fig. 1. The annual emissions by sector in China from 2000 to 2014 (PRI case). Results of total emissions in STD case and other studies are illustrated as well for comparison.

Table 1
National SO_2 and NO_X emissions of the PRI and STD cases (unit: kt). Blank values in the STD case are instances where estimated emissions are equivalent to those of the PRI case because recent standards did not apply or were not yet in effect.

		TPP	CEM	ISP	OIB	PRO	TRA	RES	Total
SO_2 (PRI)	2011	11,465	1693	2180	4422	3116	395	3731	27,002
	2012	10,531	1702	2112	4287	3301	407	3853	26,194
	2013	10,808	1826	2222	4033	3720	416	3859	26,884
	2014	9903	1839	2229	3588	3899	442	3868	25,768
SO_2 (STD)	2011					2632			26,518
	2012	9110				2809			24,281
	2013	8292		1665		2921			23,014
	2014	7308	1812	1671		3068			21,756
NO_X (PRI)	2012	10,335	3613	1503	2712	1162	7731	2424	29,481
	2013	9226	3972	1592	2722	1249	7606	2450	28,817
	2014	7421	4089	1596	2590	1277	8272	2491	27,737
NO_X (STD)	2012	9122							28,356
	2013	8482		1521					28,002
	2014	5390	3994	1525					25,540

except for official data from the Ministry of Environmental Protection (MEP, 2014). Our estimates of SO_2 emissions are lower than those by Lu et al. (2011), the inventory of Greenhouse Gas and Air Pollution Interactions and Synergies (GAINS, Klimont et al., 2009), the Regional Emission inventory in ASia (REAS, Kurokawa et al., 2013), and the Multiple Emission Inventory in China (MEIC, http://www.meicmodel.org), but larger than those reported by MEP (http://jcs.mep.gov.cn/hjzl/zkgb/). In GAINS, the FGD penetrations of the power sector were set at 28% and 56% for existing and newly-built units, respectively in 2010, lower than those in this work (86% in 2010). The relatively high emissions by REAS are attributed to the large emission factors used, although the fuel consumption is lower than that used in other inventories (Lu et al., 2011; Zhao et al., 2011). The biggest difference between this work and Lu et al. (2011) results from the estimates for industrial sources. For example, the emissions from industry in 2010 were calculated at 11.6 Mt and 20.4 Mt for the two studies, respectively, indicating less SO_2 control in industries other than the power sector assumed by Lu et al. (2011). Our estimates are close to the Emissions Database for Global Atmospheric Research (EDGAR, JRC/PBL, 2014) for earlier years, but the discrepancy increases after 2005, suggesting that the national SO_2 control measures after 2005 might not be fully considered by EDGAR. Among all the studies, the estimates from MEP are the lowest, attributed mainly to the optimistic assumption of SO_2 removal from FGD and to the omissions of emissions from rural industries and biofuel use (Zhang et al., 2009).

Our estimates in NO_X emissions are in good agreement with those by REAS, but larger than those by GAINS, EDGAR, and MEP. The discrepancies in the estimated emissions come mainly from the different emission factors applied by various studies. In this work, for example, little change in NO_X emission factors of existing power plants and industrial boilers is assumed and the average emission factor for cement production is estimated in fact to increase by 31% from 2005 to 2010. Meanwhile, in contrast, the NO_X emission factors of existing power plants were calculated to decrease 13% in GAINS. Our CO emissions are consistent with those by REAS for earlier years, but the difference becomes larger after 2005, indicating that REAS questions the full implementation of energy conservation measures. The estimates by EDGAR are extremely low compared to other studies, reflecting the large diversity in CO emission calculation, particularly for small industries, transportation, and agriculture sources. Our estimates of CO_2 emissions are generally larger than other inventories, e.g., those of the U. S. Carbon Dioxide Information Analysis Center(CDIAC, http://cdiac.ornl.gov/ftp/trends/emissions), International Energy Agency (IEA, http://www.iea.org/publications/freepublications/publication/CO2EmissionsFromFuelCombustionHighlights2014.pdf), EDGAR, MEIC, and Liu et al. (2015), attributed mainly to the use of an updated emission factor database (Zhao et al., 2012b), the use of provincial-level energy data which are indicated to be larger than national-level ones (Guan et al., 2012), and more emission sources included in this work. Besides fossil fuel combustion and calcination in cement making, emissions from biofuel use, biomass burning, and the non-combustion emissions from industrial processes other than cement are included in this work. (The latter include emissions from primary aluminum smelting in the reaction to convert aluminum oxide to aluminum metal.)

3.2. Comparisons of emissions and VCDs from satellite observations

Fig. 2 shows the inter-annual trends in emissions normalized to the level of 2005 and the 12-month moving averages of tropospheric VCDs from satellite observations normalized to the level of June 2005, for mainland China between 2005 and 2014. In general, the correlations between the trends in emissions and VCDs are better for NO_X than SO_2 or CO.

Although the bottom-up SO_2 emissions and VCDs match well for certain periods, e.g., both were found to decline in 2008–2009 attributed to reduced emission factors from FGD use and the limited economic activities for the Beijing Olympics and the subsequent global financial crisis (Lin et al., 2013), there is clear difference in the inter-annual trends between them. The SO_2 VCDs increased 4% from 2005 to 2011 and then decreased 28% from 2011 to 2014, while the SO_2 emissions (PRI case) decreased 7% from 2005 to 2011 and changed only slightly from 2011 to 2014. The result thus indicates that growth in SO_2 VCDs were found during the period for which emissions were estimated to decline, and significant reduction in VCD occurred when only limited emission abatement was achieved. Various reasons may contribute to the inconsistency, as described below.

Uncertainties in emission estimation may be partly responsible for the inconsistency. During the 11th FYP period, the fraction of installed capacity with FGD systems in power sector increased sharply from 13% in 2005 to 86% in 2010, and the SO_2 emission factor for entire sector was estimated to decline 61%, with the average removal efficiency of FGD set at 75% (Zhao et al., 2013). A large uncertainty, nevertheless, existed in this parameter due to unclear operation of FGD systems, and the emissions maybe larger than expected if poor management of FGD motivated by economic incentives prevailed (Zhao et al., 2013). Even with limited additional potential for FGD, the drop in SO_2 VCD after 2012 could partly result from the improved running of FGD systems. In September 2013, for example, the Chinese State Council issued the National Action Plan on Prevention and Control of Air Pollution, requiring elevated controls of pollutant emissions (Zhao et al., 2014). The benefits of the plan on emission abatement, however, could not be fully quantified in this work attributed largely to lack of updated measurement data on typical emissions sources. Thus overestimation on emissions for 2013 and 2014 might occur. As shown in Fig. 2, the SO_2 emissions of the STD case are in better agreement with VCDs than those of the PRI case, suggesting STD case is a better representation of implementation of post-2010 emission standards than the PRI case. In addition, the faster decrease in SO_2 VCDs than emissions (in the STD case) from 2011 to 2014 could also result from the calculation of emission factors. In the STD case, the limits of flue gas concentrations set by the standards (e.g., 100 SO_2 mg/m^3 for power plants) are directly taken to estimate the average emission factors, due to lack of actual flue gas measurement data. If a given plant strictly meets the standard all of the time, however, the annual average concentration in the flue gas must be lower than the standard limit, since the real-time concentrations in the flue gas

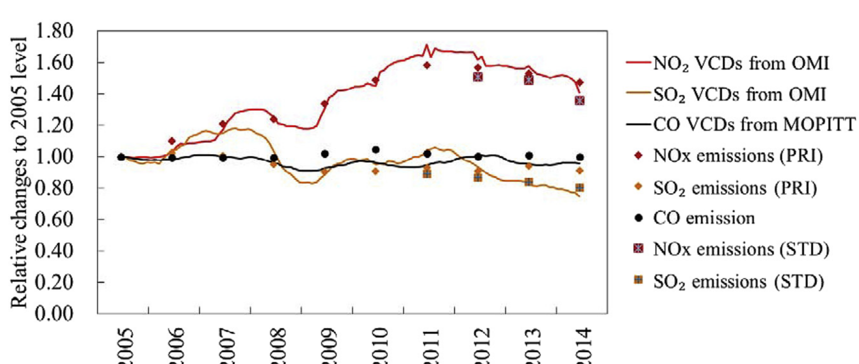

Fig. 2. The inter-annual trends in satellite-based VCDs for the mainland China and national bottom-up emissions (in both PRI and STD cases) from 2005 to 2014. All data are normalized to the year 2005.

vary significantly, leading to emissions below the standards. To better quantify the emissions from bottom-up methods, therefore, data from real-time measurements should be applied once they are available. Besides the emissions, the fast decline in SO_2 VCDs might result partly from enhanced atmospheric oxidation capacity that accelerates the conversion of SO_2 to sulfate. As reported by MEP, the annual average of the daily maximum 8-h mean O_3 concentrations for the 74 key cities in China has increased by 8% between 2013 and 2015 (data source: http://jcs.mep.gov.cn/hjzl/zkgb/2014zkgb/201506/t20150608_303142.htm), and more depletion of SO_2 due to the enhanced formation of sulfate may have occurred. Finally, the weakness and uncertainty from satellite retrievals may also contribute to the inconsistencies between the bottom-up emissions and VCD trends, e.g., densities through the whole atmospheric column instead of concentrations at the surface could not fully represent the anthropogenic emissions mainly from surface.

The NO_2 VCDs increased 71% from 2005 to 2011 and then decreased 18% from 2011 to 2014, consistent with the bottom-up emission estimates for NO_X. Thus the reduced VCDs from satellite observations support the estimation of strong emission abatement during the 12th FYP period. Combining the inter-annual trends of SO_2 and NO_X, it can be found that the estimated emissions in the STD case are in better agreement with the satellite observation for both species (quantitative analysis is shown in Table 2 and will be discussed below), suggesting that implementation of emission controls since 2010 in China has been more transparent and is therefore easier to track in emission inventory studies.

The CO VCDs decreased 4% from 2005 to 2012 and the inter-annual trend is in general consistent with the bottom-up emissions. Discrepancies are mainly found between 2009 and 2011, in which the emissions are estimated to have increased while a relatively stable trend was found for VCDs. Different from SO_2 or NO_X, CO emissions result mostly from incomplete combustion at small industrial and residential sources, and the improvement of energy efficiency for these sources is relatively difficult to be fully tracked using bottom-up methods (Streets et al., 2006) leading to overestimation of emission levels or growth. Such discrepancies can be reduced through emission estimation using inverse methods that incorporate satellite VCDs and chemical transport simulation (Yumimoto et al., 2014). Moreover, estimated CO VCDs declined more significantly during the 11th FYP period (2006–2010) than the 12th FYP (2011–2014), in contrast to SO_2. As mentioned earlier, the main measures of air pollution control in the 11th FYP period in China included replacement of small industrial sources with large ones and application of FGD systems in the power sector. The former would immediately have an effect on combustion efficiency and thereby CO levels, while the latter would not necessarily reduce SO_2 emissions, if the FGD systems were not properly operated, as discussed earlier. In the most recent years, however, most small industrial plants had already been shut down, leaving little room for further improvement in energy efficiency, while the improved SO_2 removal rates of FGD due to implementation of emission standards started to play a crucial role in cutting SO_2 emissions.

Inter-annual trends in emissions, VCDs, and a number of social, economic, and energy indicators between 2005 and 2014 are shown in Fig. S2 in the supplement. The trend in NO_X emissions is more consistent with all the indicators than SO_2, due mainly to the abatement of SO_2 emissions from FGD use. As shown in Table 2, both NO_X emissions and NO_2 VCDs have the strongest correlations with total coal consumption among all the indicators, implying that coal consumption is the main driving force of NO_X pollution in China. The agreement, however, is found to be worse after 2012 as shown in Fig. S2, reflecting reduced NO_X emissions from SCR/SNCR use. Although transportation is identified as an important NO_X source in the bottom-up inventory, the correlation between NO_X emissions and the vehicle population is relatively poor, since the staged enforcement of vehicle emission standards lead to slower increases in NO_X emissions from transportation than the growth of the vehicle population.

4. Varied control effects by region and source

4.1. Spatial distributions of NO_2 and SO_2 and implications for pollution sources

To examine the regional differences in VCDs and emissions, their inter-annual trends for various regions of the country are compared in Fig. S4 in the supplement. The regions for emissions include four groups of provinces, specifically: (1) the Jing-Jin-Ji (JJJ) provinces including Beijing, Tianjin, and Hebei; (2) Yangtze River Delta (YRD) provinces including Jiangsu, Zhejiang, Anhui, and Shanghai; (3) Guangdong (containing the Pearl River Delta, PRD); and (4) Sichuan (containing part of the Sichuan Basin, SB). The regions for VCDs include the former four groups of provinces and western China (WC) where economy is less developed, as shown in Fig. S3 in the supplement.

In general, similar trends in emissions and VCDs are found by region. SO_2 emissions in JJJ and YRD are estimated to have declined faster than those in western provinces during the 11th FYP (Fig. S4b). Accordingly, a decreasing trend in SO_2 VCDs is found across the country except for WC (Fig. S4a). The results likely reflect better implementation of SO_2 control through FGD use in developed regions. Similarly, NO_2 VCDs in JJJ increased fastest among all the regions before 2012 and then decreased, while those in WC kept growing (Fig. S4c). This suggests the effectiveness of SCR/SNCR use on NO_X abatement in JJJ, as illustrated by the emission trends (Fig. S4d). Specifically, NO_2 VCDs in Guangdong started to decline after 2007, while NO_X emissions in Guangdong increased 37% from 2005 to 2012 (Fig. S4c and d). The inconsistency may result partly from the increased atmospheric oxidation over the region. As reported by the Department of Environmental Protection of Guangdong (http://www.gdep.gov.cn), enhanced O_3 in PRD was observed during 2006–2011, which may have consumed large amounts of NO_2.

Figs. 3 and 4 illustrate the spatial distribution of SO_2 and NO_2 VCDs for various years, respectively (see the results based only on data for May–September in Figs. S6 and S7 in the supplement). High SO_2 VCDs appeared in eastern China with large densities of industrial activity, and in SB with very high sulfur content of coals. NO_2 pollution was more serious in eastern China and PRD. Besides intensive coal combustion, transportation also contributed

Table 2
Correlation coefficients between NO_2 VCDs, NO_X emissions, and economic indicators.

	Industrial GDP	Vehicle population	Total coal consumption	Coal-fired power generation	Emissions (PRI)	Emissions (STD)
VCDs from OMI	0.866	0.796	0.936	0.903	0.976	0.979
Emissions (PRI)	0.913	0.855	0.965	0.945	-	-
Emissions (STD)	0.828	0.752	0.910	0.877	-	-

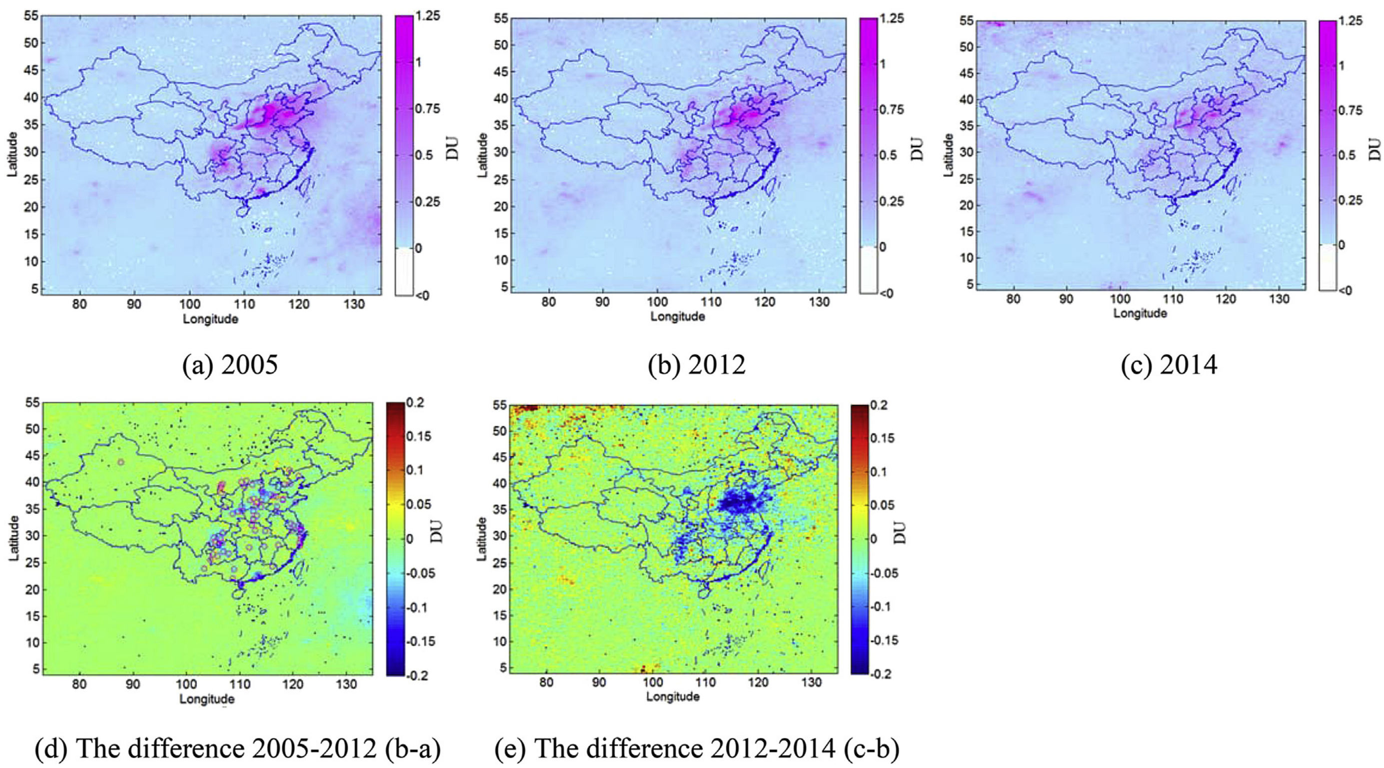

Fig. 3. Spatial distribution of SO2 VCDs in 2005 (a), 2012 (b) and 2014(c), and the inter-annual variation between 2005 and 2012 (d) and that between 2012 and 2014 (e). The locations of big power plants are indicated by the circles in panel (d).

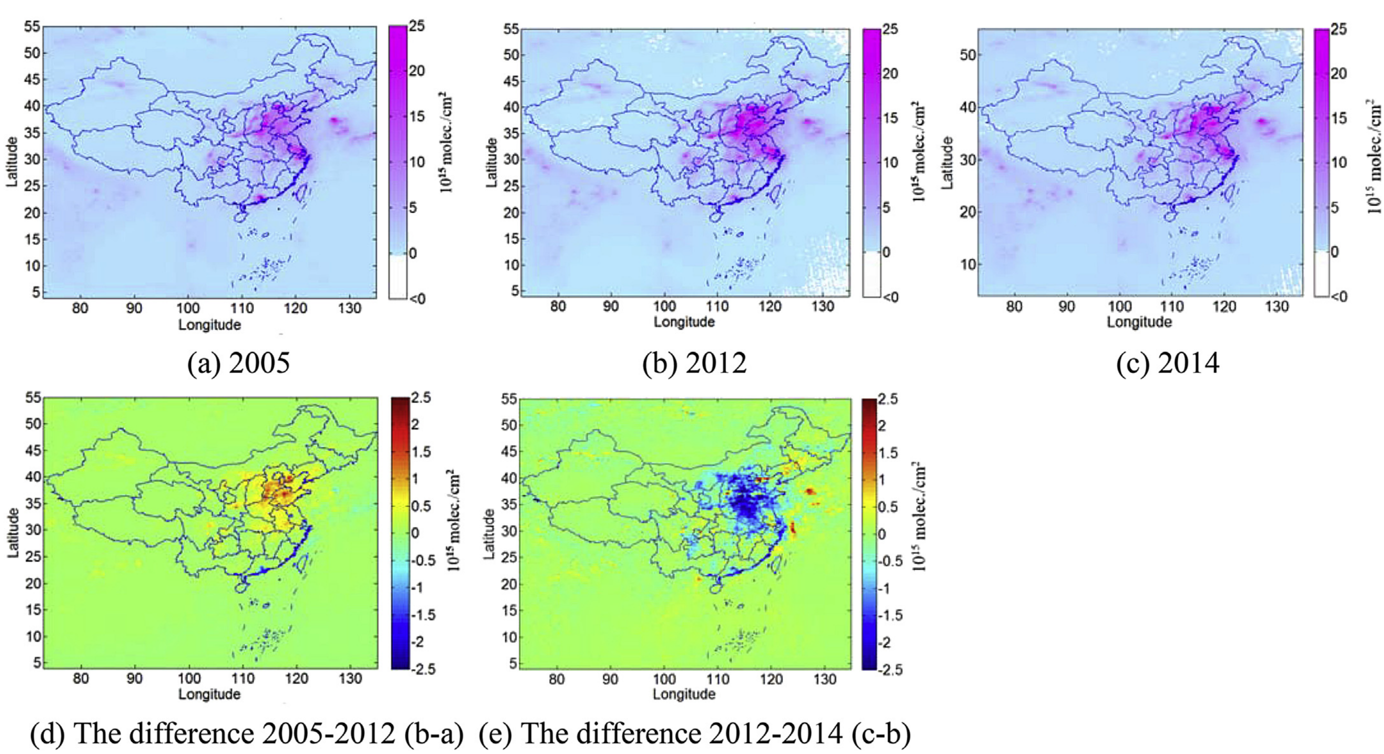

Fig. 4. Spatial distribution of NO2 VCDs in 2005 (a), 2012 (b) and 2014(c), and the inter-annual variation between 2005 and 2012 (d) and that between 2012 and 2014 (e).

significantly to NO_X emissions in those developed regions, as discussed later in Section 4.2. Fig. 3d shows the relative changes in SO_2 VCDs from 2005 to 2012. Decreased SO_2 can be found in high polluted areas including south JJJ, central YRD, and PRD regions, attributed mainly to emission abatement from TPP. As shown in Fig. S5 in the supplement, SO_2 emissions from the coal-fired power sector are estimated to have declined 41% from 2005 to 2010, using a detailed unit-based calculation method (Zhao et al., 2008). The reduction in SO_2 VCDs agreed well with the locations of big power units (Fig. 3d). More significant reduction in SO_2 VCDs occurred in highly polluted areas from 2012 to 2014 (Fig. 3e), implying improved FGD operations at power and iron & steel plants, as well as the enforcement of tightened emission standards. While the average SO_2 VCDs of May–September were clearly lower (Fig. S6a–c), similar spatial pattern and temporal trend could be found with those of full year (Fig. S6d–e). The NO_2 VCDs increased from 2005 to 2012 in most part of eastern China but declined in Shanghai and the PRD region (Fig. 4d and Fig. S7d). To improve air quality in developed cities, some industries with relatively large emissions have gradually been moved out from urban to surrounding areas, leading to reduced emissions and thereby VCDs in mega cities. Decreased NO_2 VCDs in highly polluted areas can be found after 2012 indicating the NO_X control in those regions started to take effect. Comparing Figs. 3d, 4d and 4e, it can be seen that the abatement of NO_2 in heavy polluted eastern China was later than that of SO_2, due to a different emission control schedule and actions of the country in the 11th and 12th FYP periods. The earlier promotion of FGD systems than SCR/SNCR systems in the power sector led to reduced SO_2 emissions in eastern China while NO_X kept growing before 2010.

The inter-annual trends in VCDs in mega cities Beijing and Shanghai as well as those in their surrounding provinces (Hebei-Tianjin, HT and Jiangsu-Zhejiang-Anhui, JZW) are analyzed and shown in Fig. 5 (see Fig. S3 for the locations of these regions and provinces). The NO_2 VCDs in Shanghai started to decrease in 2008, while those in JZW kept growing by 43% from 2005 to 2011 and then decreased 20% from 2011 to 2014. Little correlation is found between VCDs of the two regions. In contrast, the NO_2 VCDs in Beijing and HT increased 32% and 63.3% from 2005 to 2012, followed by reductions of 14% and 16% from 2012 to 2014, respectively. Given that NO_X emissions in Beijing are estimated to have declined from 2005, emissions from surrounding areas would be more influential in NO_2 levels for Beijing than those for Shanghai. Similar results were provided by numerical simulation studies. With a Daily Emission estimates Constrained by Satellite Observations (DECSO) algorithm, for example, Mijling et al. (2013) estimated that at least 28% of Beijing's NO_2 came from Hebei and Tianjin and overall 12% was imported from more remote provinces, while Cheng et al. (2011) found that non-local primary NO_X contributed less to NO_2 level in Shanghai at 16% and 11% in January and July, respectively, using CALPUFF model. For SO_2, the correlation between VCDs in Beijing and HT is better ($R = 0.93$) than that between Shanghai and JZW ($R = 0.82$). The larger reduction in VCDs in Shanghai is found than that in JZW from 2005 to 2014, consistent with the inter-annual trends in emissions. The SO_2 emissions in Shanghai and JZW are estimated to have declined by 58% and 27%, respectively, indicating more effective emission controls for industrial sources in developed cities.

4.2. Growing importance of transportation

The bottom-up emission inventory reveals that SO_2 results mainly from stationary combustion sources including power and industrial boilers while NO_X from both stationary and mobile sources. Given the similar lifetimes and emission intensities of SO_2 and NO_2, elevated contributions from transportation to air quality can be inferred if relatively high ratios of NO_2 to SO_2 VCDs is found. Shown in Fig. 6a–c are the spatial distributions of NO_2 to SO_2 VCD ratios for various years over the country. In 2005, large ratios appeared in developed regions such as Beijing, PRD, and Zhejiang province, consistent with the provincial NO_X emission intensities of transportation as illustrated in Fig. S8a in the supplement. The fractions of NO_X emissions from transportation in JJJ (39%), YRD (27%), and Guangdong province (29%) were larger than the national average level of 24% (see Fig. S3 for the locations of different regions), and the fractions reached 40% and 46% for Beijing and Shanghai, respectively. Even with staged implementation of tightened emission standards for on-road vehicles, an enhanced emission intensity of transportation is estimated from 2005 to 2012 (Fig. S8a and b). The fraction of NO_X emissions from transportation grew to 30% for the whole country in 2014, and the values reached 44%, 55%, and 33% for Beijing, Shanghai, and Guangdong, respectively. Dramatic growth in the on-road vehicle populations and non-road sources subject to less stringent regulation is believed to be the main reason. The areas with large NO_2 to SO_2 VCD ratio have extended over time to the YRD region (Fig. 6b), and then to the whole of eastern China, SB, and several provincial capitals in central and western China (Fig. 6c). Based on a combination of bottom-up emissions and information from satellite observations, therefore, transportation is believed to play an increasingly important role in regional NO_2 pollution, especially when emissions from stationary sources are gradually controlled through increased penetration of SCR/SNCR.

In the transportation category, the fuel consumption and emissions from ocean shipping have been growing increasingly important. In Shanghai, as an example, about 12%, 8%, and 5% of total SO_2, NO_X, and primary $PM_{2.5}$ emissions originated in its harbor in 2010 (Fu et al., 2012), one of the largest ocean ports in China. Shown in Fig. S9a and b in the supplement are the inter-annual changes of NO_2 VCDs at the main ocean ports in the YRD and Bohai Gulf between 2012 and 2014, respectively. Increases in NO_2 VCDs are found in most ports except Zhoushan, consistent with the growth of activity levels in ocean shipping. From 2012 to 2014, the cargo volumes and container throughput increased 3–19% and 8–31%, respectively, for the six ports shown in the figure (Shanghai, Zhoushan, Dalian, Yantai, Weihai and Tianjin). Since Zhoushan harbor is close to many highly polluting industries, the growth in emissions from ships maybe partly offset by declining emissions from industries. As illustrated in Fig. S10, the ratio of ships to total NO_X emissions (STD case for 2012–2014) kept growing from 2005 to 2014 in given provinces containing big ports, including Shanghai and Zhejiang in the YRD and Liaoning by Bohai Gulf (see Fig. S9 for the locations of these provinces). Different from on-road vehicles, few measures have been taken to reduce atmospheric pollutants from ship emissions. The problem has been noticed by the government and new emission standards for ships are under discussion and expected to be issued soon (MEP and GAQSIQ, 2015).

4.3. Spatial pattern of CO and its dependence on iron & steel production

Fig. 7a–c displays spatial distributions of CO VCDs in 2005, 2010 and 2014, respectively (see the results based only on data for May–September in Fig. S11a–c in the supplement). High VCDs appeared in eastern China, PRD, and SB, similar to those for SO_2 and NO_X. As shown in Fig. 7d, the VCDs are found to have declined significantly from 2005 to 2010 over these highly polluted areas, with an exception at the Tangshan region in Hebei province, indicating achievements of CO emission control resulting mainly from closure of small industrial and residential combustors with low energy efficiencies in those areas. Meanwhile, much less CO VCD reduction is found for WC, the area with the least developed economy and air pollution. In this region, residential fossil and biofuel combustion instead of industrial boilers or kilns are the dominant source of CO, and few control measures have been enacted for those sources. This is consistent with the comparison of

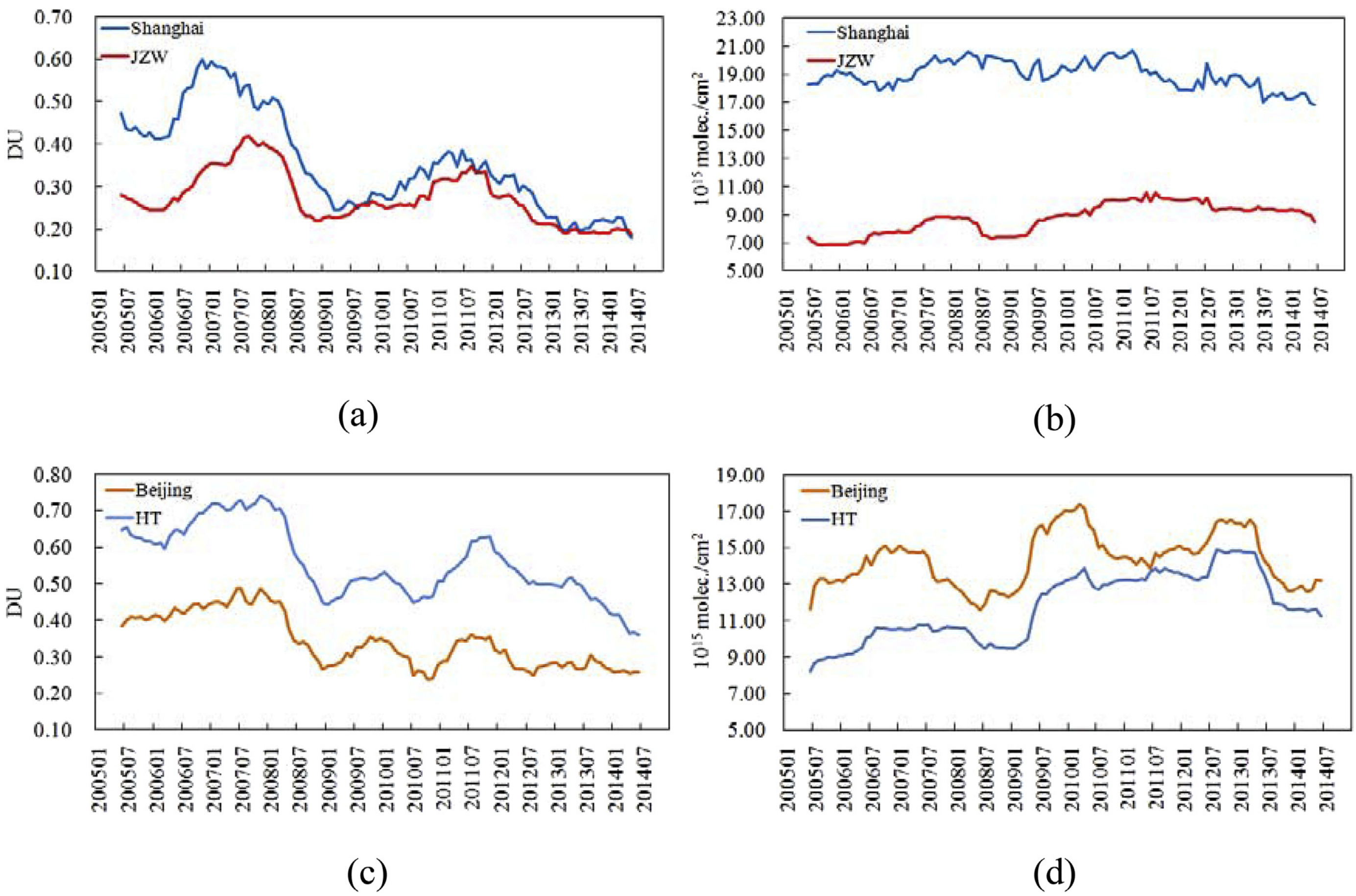

Fig. 5. The inter-annual trends in SO2 VCDs of Shanghai and Jiangsu-Zhejiang-Anhui (JZW) (a), NO_2 VCDs in Shanghai and JZW (b), SO2 VCDs in Beijing and Hebei-Tianjin (HT) (c), and NO_2 VCDs in Beijing and HT (d).

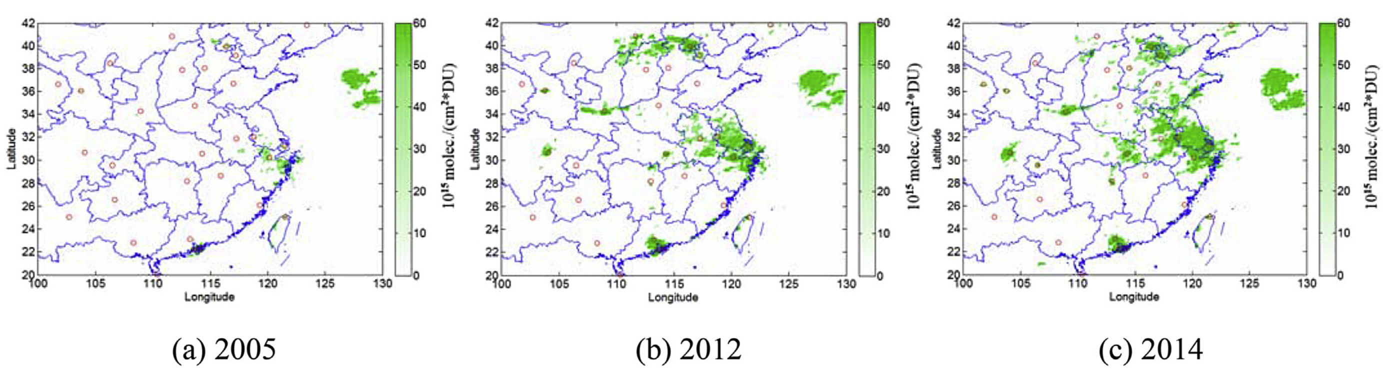

Fig. 6. The NO2 to SO2 VCD ratios in 2005, 2012 and 2014 respectively. To highlight the relatively high polluted region, the areas with SO2 VCDs under 0.05 DU or NO2 VCDs under 5×10^{15} molecule/cm^2 are excluded and only the ratios larger than 40×10^{15} molecule/(cm^2·DU) are displayed. The circles represent provincial capital cities.

emissions and VCDs by region (Fig. S4e and f). Similar pattern was found when the data of May–September were used, with an exception that the inter-annual variation for PRD was less conclusive due mainly to lack of valid data (Fig. S11d). From 2010 to 2014, weaker progress of CO control is found in most of eastern China, as most small industrial facilities had been shut down, and few new measures or standards targeting CO were issued during the 12th FYP (Fig. 7e and Fig. S11e).

Iron & steel production (ISP) is another important source of CO and may dominate emissions around the Tangshan region. Tangshan is the Chinese city with the largest iron & steel industry, manufacturing about half of the iron & steel products of Hebei province. From 2005 to 2010, the iron & steel output in Hebei increased by 95% while the CO emissions from ISP increased much slower, at 24%, reflecting the benefits of emission control in the sector. The share of total provincial anthropogenic emissions of CO from ISP grew from 39% to 45%, as shown in Fig. 7f. From 2010 to 2014, CO emissions from ISP in Hebei are estimated to have declined 16% and its share of all anthropogenic CO in the province stopped growing, due largely to slower growth of steel output after

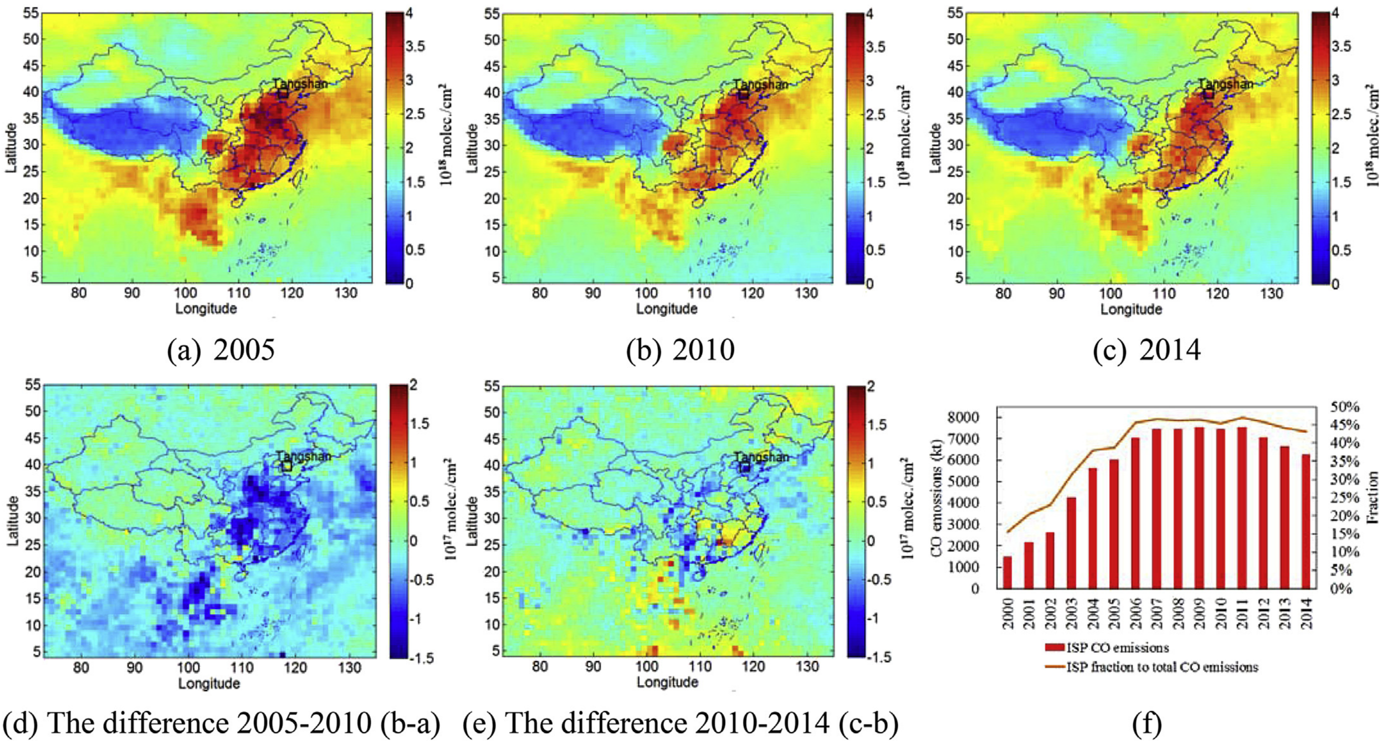

Fig. 7. Spatial distribution of CO VCDs in 2005 (a), 2010 (b) and 2014 (c), and the inter-annual variation between 2005 and 2010 (d) and that between 2010 and 2014 (e). The inter-annual trends in CO emissions from ISP in Hebei province and the shares of ISP to total provincial anthropogenic emissions are shown in panel (f).

2010 (37% from 2010 to 2014) and to continuously improved recycling of flue gas in blast furnace in pig iron production and in basic oxygen furnaces in steel making. As shown in Fig. 7d and e, accordingly, the VCDs over the Tangshan region were found to increase from 2005 to 2010 and to decrease after 2010, suggesting the crucial role of ISP in determining ambient CO levels.

5. Conclusions

Indicated by inter-annual analysis of emissions and VCDs from satellite observations, China's efforts in air pollution control have been taking effect, although differing by region and species across the country. Coal consumption dominated the growth of NO_X emissions and NO_2 VCDs before 2012, followed by reduced emissions and VCDs attributed mainly to increased and improved use of SCR/SNCR controls in the power sector. Despite faster penetration of FGD systems before 2010, larger benefits in SO_2 abatement are found for 2012–2014, resulting from the improved running of FGD systems in the power sector and better implementation of new emission standards across sectors. Inter-annual variability of CO is small, and reduced VCDs result from improved energy efficiency as suggested by decreased emission ratios of CO to CO_2. In most cases, larger reduction of VCDs of gaseous pollutants have been found in areas with relatively high pollution levels, such as the eastern China and PRD regions. With emissions from industrial sources incrementally controlled, transportation is playing an increasingly important role in regional air pollution.

Acknowledgement

This work was sponsored by the Natural Science Foundation of China (41575142), Natural Science Foundation of Jiangsu (BK20140020), Jiangsu Science and Technology Support Program (SBE2014070918), and Special Research Program of Environmental Protection for Commonweal (201509004). We would like to acknowledge the free use of tropospheric NO2 column data from TEMIS, and PBL SO2 column data and total CO column data from NASA. Thanks should also go to two anonymous reviewers for their very valuable comments to improve this work.

Appendix A. Supplementary data

Supplementary data related to this article can be found at http://dx.doi.org/10.1016/j.atmosenv.2016.04.013.

References

Cheng, Z., Chen, C.H., Huang, C., Huang, H.Y., Li, L., Wang, H.L., 2011. Trans-boundary primary air pollution between cities in the Yangtze River Delta. Acta Sci. Circumstantiae 31 (4), 686–694.

Cofala, J., Amann, M., Klimont, Z., Kupiainen, K., Hoglund-Isaksson, L., 2007. Scenarios of global anthropogenic emissions of air pollutants and methane until 2030. Atmos. Environ. 41, 8486–8499.

Deeter, M.N., Martínez-Alonso, S., Edwards, D.P., Emmons, L.K., Gille, J.C., Worden, H.M., Pittman, J.V., Daube, B.C., Wofsy, S.C., 2013. Validation of MOPITT Version 5 thermal-infrared, near-infrared, and multispectral carbon monoxide profile retrievals for 2000-2011. J. Geophys. Res. Atmos. 118, 6710–6725.

Fu, Q., Shen, Y., Zhang, J., 2012. On the ship pollutant emission inventory in Shanghai port. J. Saf. Environ. 12, 57–64.

Guan, D.B., Liu, Z., Geng, Y., Lindner, S., Hubacek, K., 2012. The gigatonne gap in China's carbon dioxide inventories. Nat. Clim. Change 2, 672–675.

Joint Research Centre (JRC)/Netherlands Environmental Assessment Agency (PBL), 2014. Emission Database for Global Atmospheric Research (EDGAR), Release Version 4.2. Available online at: http://edgar.jrc.ec.europa.eu.

Klimont, Z., Cofala, J., Xing, J., Wei, W., Zhang, C., Wang, S., Jiang, K., Bhandari, P., Mathur, R., Purohit, P., Rafaj, P., Chambers, A., Amann, M., Hao, J., 2009. Projections of SO_2, NOx and carbonaceous aerosols emissions in Asia. Tellus B 61, 602–617.

Kurokawa, J., Ohara, T., Morikawa, T., Hanayama, S., Janssens-Maenhout, G., Fukui, T., Kawashima, K., Akimoto, H., 2013. Emissions of air pollutants and greenhouse gases over Asian regions during 2000-2008: regional Emission inventory in Asia (REAS) version 2. Atmos. Chem. Phys. 13, 11019–11058.

Lee, C., Martin, R.V., van Donkelaar, A., O'Byrne, G., Krotkov, N., Richter, A., Huey, L.G., Holloway, J.S., 2009. Retrieval of vertical columns of sulfur dioxide

from SCIAMACHY and OMI: air mass factor algorithm development, validation, and error analysis. J. Geophys. Res. 114, D22303. http://dx.doi.org/10.1029/2009jd012123.
Lei, Y., Zhang, Q., Nielsen, C.P., He, K.B., 2011. An inventory of primary air pollutants and CO_2 emissions from cement industry in China, 1990–2020. Atmos. Environ. 45, 147–154.
Lin, J., Pan, D., Zhang, R., 2013. Trend and interannual variability of Chinese air pollution since 2000 in association with socioeconomic development: a brief overview. Atmos. Ocean. Sci. Lett. 6, 84–89.
Lin, J., Martin, R.V., Boersma, K.F., Sneep, M., Stammes, P., Spurr, R., Wang, P., van Roozendael, M., Clémer, K., Irie, H., 2014. Retrieving tropospheric nitrogen dioxide from the Ozone Monitoring Instrument: effects of aerosols, surface reflectance anisotropy, and vertical profile of nitrogen dioxide. Atmos. Chem. Phys. 14, 1441–1461.
Liu, Z., Guan, D., Wei, W., Davis, S.J., Ciais, P., Bai, J., Peng, S., Zhang, Q., Hubacek, K., Marland, G., Andres, R.J., Crawford-Brown, D., Lin, J., Zhao, H., Hong, C., Boden, T.A., Feng, K., Peters, G.P., Xi, F., Liu, J., Li, Y., Zhao, Y., Zeng, N., He, K., 2015. Reduced carbon emission estimates from fossil fuel combustion and cement production in China. Nature 524, 335–338.
Lu, Z., Zhang, Q., Streets, D.G., 2011. Sulfur dioxide and primary carbonaceous aerosol emissions in China and India, 1996-2010. Atmos. Chem. Phys. 11, 9839–9864.
Mijling, B., van der, A.R.J., Zhang, Q., 2013. Regional nitrogen oxides emission trends in East Asia observed from space. Atmos. Chem. Phys. 13, 12003–12012.
Ministry of Environment Protection of China (MEP), 2011. Report on Environmental Quality in China, 2010. Available online at: http://jcs.mep.gov.cn/hjzl/zkgb/2010zkgb/201106/t20110602_211579.htm.
Ministry of Environment Protection of China (MEP), 2014. Report on Environmental Quality in China, 2013. Available online at: http://jcs.mep.gov.cn/hjzl/zkgb/2013zkgb/201406/t20140605_276521.htm.
Ministry of Environment Protection of China (MEP), General Administration of Quality Supervision, Inspection and Quarantine of China (GAQSIQ), 2015. Limits and Measurement Methods for Exhaust Pollutants from Marine Compression Ignition Engines (China I and II).
National Bureau of Statistics (NBS), 2013a. China Energy Statistical Yearbook 2000-2012. China Statistics Press, Beijing, China.
National Bureau of Statistics (NBS), 2013b. China Industry Economy Statistical Yearbook 2000-2012. China Statistics Press, Beijing, China.
National Bureau of Statistics (NBS), 2014. China Statistical Yearbook 2000-2014. China Statistics Press, Beijing, China.
Richter, A., Burrows, J.P., Nuss, H., Granier, C., Niemeier, U., 2005. Increase in tropospheric nitrogen dioxide over China observed from space. Nature 437, 129–132.
Streets, D.G., Bond, T.C., Carmichael, G.R., Fernandes, S.D., Fu, Q., He, D., Klimont, Z., Nelson, S.M., Tsai, N.Y., Wang, M.Q., Woo, J.-H., Yarber, K.F., 2003. An inventory of gaseous and primary aerosol emissions in Asia in the year 2000. J. Geophys. Res. 108 (D21), 8809. http://dx.doi.org/10.1029/2002jd003093.
Streets, D.G., Zhang, Q., Wang, L., He, K., Hao, J., Wu, Y., Tang, Y., Carmichael, G.R., 2006. Revisiting China's CO emissions after the transport and chemical evolution over the pacific (TRACE-P) mission: synthesis of inventories, atmospheric modeling, and observations. J. Geophys. Res. 111, D14306. http://dx.doi.org/10.1029/2006jd007118.
Wang, S., Hao, J., 2012. Air quality management in China: issues, challenges, and options. J. Environ. Sci. 24, 2–13.
Worden, H.M., Deeter, M.N., Frankenberg, C., George, M., Nichitiu, F., Worden, J., Aben, I., Bowman, K.W., Clerbaux, C., Coheur, P.F., de Laat, A.T.J., Detweiler, R., Drummond, J.R., Edwards, D.P., Gille, J.C., Hurtmans, D., Luo, M., Martínez-Alonso, S., Massie, S., Pfister, G., Warner, J.X., 2013. Decadal record of satellite carbon monoxide observations. Atmos. Chem. Phys. 13, 837–850.
Wu, Y., Zhang, S., Li, M., Ge, Y., Wu, J., Zhou, Y., Xu, Y., Hu, J., Liu, H., Fu, L., He, K., Hao, J., 2012. The challenge to NO_X emission control for heavy-duty diesel vehicles in China. Atmos. Chem. Phys. 12, 9365–9379.
Xu, Y., 2011. Improvements in the operation of SO_2 scrubbers in China's coal power plants. Environ. Sci. Technol. 45, 380–385.
Yao, Z., Huo, H., Zhang, Q., Streets, D.G., He, K., 2011. Gaseous and particulate emissions from rural vehicles in China. Atmos. Environ. 45, 3055–3061.
Yumimoto, K., Uno, I., Itahashi, S., 2014. Long-term inverse modeling of Chinese CO emission from satellite observations. Environ. Pollut. 195, 308–318.
Zhang, Q., Streets, D.G., Carmichael, G.R., He, K., Huo, H., Kannari, A., Klimont, Z., Park, I., Reddy, S., Fu, J.S., Chen, D., Duan, L., Lei, Y., Wang, L., Yao, Z., 2009. Asian emissions in 2006 for the NASA INTEX-B mission. Atmos. Chem. Phys. 9, 5131–5153.
Zhang, Q., He, K., Huo, H., 2012. Cleaning China's air. Nature 484, 161–162. http://dx.doi.org/10.1038/484161a.
Zhao, Y., Wang, S., Duan, L., Lei, Y., Cao, P., Hao, J., 2008. Primary air pollutant emissions of coal-fired power plants in China: current status and future prediction. Atmos. Environ. 42, 8442–8452.
Zhao, Y., Nielsen, C.P., Lei, Y., McElroy, M.B., Hao, J., 2011. Quantifying the uncertainties of a bottom-up emission inventory of anthropogenic atmospheric pollutants in China. Atmos. Chem. Phys. 11, 2295–2308.
Zhao, Y., Nielsen, C.P., McElroy, M.B., Zhang, L., Zhang, J., 2012a. CO emissions in China: uncertainties and implications of improved energy efficiency and emission control. Atmos. Environ. 49, 103–113.
Zhao, Y., Nielsen, C.P., McElroy, M.B., 2012b. China's CO_2 emissions estimated from the bottom up: recent trends, spatial distributions, and quantification of uncertainties. Atmos. Environ. 59, 214–223.
Zhao, Y., Zhang, J., Nielsen, C.P., 2013. The effects of recent control policies on trends in emissions of anthropogenic atmospheric pollutants and CO_2 in China. Atmos. Chem. Phys. 13, 487–508.
Zhao, Y., Zhang, J., Nielsen, C.P., 2014. The effects of energy paths and emission controls and standards on future trends in China's emissions of primary air pollutants. Atmos. Chem. Phys. 14, 8849–8868.